JOURNAL OF SOLID STATE CHEMISTRY **130,** 272–276 (1997)
ARTICLE NO. SC977363

The Structural Characterization of Tin- and Titanium-Doped α-Fe_2O_3 Prepared by Hydrothermal Synthesis

Frank J. Berry,* Colin Greaves,† Julia G. McManus,* Michael Mortimer,* and Gordon Oates*

** Department of Chemistry, The Open University, Walton Hall, Milton Keynes MK7 6AA, United Kingdom; and † School of Chemistry, The University of Birmingham, Edgbaston, Birmingham B15 2TT, United Kingdom*

Received February 26, 1997; accepted February 27, 1997

The structural characteristics of tin- and titanium-doped α-Fe_2O_3 prepared by hydrothermal methods have been investigated by Rietveld structure refinement of the X-ray powder diffraction data. The analysis reveals that the dopant ions adopt two distinct sites: in addition to partially substituting at the octahedral Fe sites, they also occupy the interstitial octahedral sites which are vacant in the α-Fe_2O_3 structure. The structural model deduced involves clusters of three substituted cations and is rational in that it represents microstructural regions of the rutile structure within a matrix of α-Fe_2O_3.

INTRODUCTION

The effect of metal doping, including such metals as titanium (1, 2), tin (3–7), manganese (8), aluminium (9, 10), gallium (11), and indium (12), on the electrical, magnetic, and other physical properties of α-Fe_2O_3 (hematite) has been an area of active investigation for some time. It is generally proposed that the dopant metal ions substitute for Fe^{3+} in the corundum-related structure of α-Fe_2O_3 with the consequent formation of cationic and anionic vacancies. In terms of this model it is expected that the difference in ionic radius between the dopant metal ion and that for Fe^{3+} will influence the structural characteristics and phase behavior of the doped system. In the present work we report on an investigation by X-ray diffraction, with Rietveld structure refinement, of the structures of tin- and titanium-doped α-Fe_2O_3. Samples of both types of doped material were prepared by hydrothermal synthesis and were found to give well-resolved XRD patterns.

EXPERIMENTAL

The compounds of compositions α-$Fe_{1.88}Sn_{0.12}O_3$, α-$Fe_{1.67}Sn_{0.33}O_3$, and α-$Fe_{1.78}Ti_{0.22}O_3$ were prepared by precipitating aqueous mixtures of iron(III) chloride hexahydrate and tin(IV) chloride (or titanium(IV) chloride) with aqueous ammonia and hydrothermally processing the precipitates in a Teflon-lined autoclave at 200°C and 15 atm pressure for 5 hr. The products were removed by filtration and washed with 95% ethanol until no chloride ions were detected by silver nitrate solution. The products were dried under an infrared lamp.

X-ray powder diffraction (XRD) data were recorded with a Siemens D5000 diffractometer in reflection mode using Cu$K\alpha$ radiation. The program FULLPROF (13) was used for Rietveld refinement and simulation of patterns for specific structural models.

RESULTS AND DISCUSSION

XRD patterns from samples containing tin or titanium generally showed marked differences from the experimental and simulated patterns of pure α-Fe_2O_3. In particular, the relative intensity of the two peaks in the region 33°–36° 2θ—(104) and (110) reflections—was often reversed, although the precise intensities from a given sample were found to vary substantially depending on the manner of sample packing prior to data collection. This was strongly suggestive of pronounced preferred orientation in the samples typical of an acicular habit, with elongation along $\langle 001 \rangle$ providing an intensity enhancement of the ($hk0$) reflections. Accordingly, allowance for such effects was an important consideration for the examination of possible structural models for the substituted α-Fe_2O_3 samples.

The structure of α-Fe_2O_3 has Fe^{3+} ions distributed in an ordered fashion in 2/3 of the octahedral sites within a framework of hexagonally close-packed O^{2-} ions. Chains of face-sharing octahedra are directed along the c axis, and the Fe^{3+} ions within each chain form pairs as shown in Fig. 1a. Given the preference of Sn^{4+} for octahedral coordination, it seemed likely that the defect structure involves substitution of Sn^{4+} for Fe^{3+}, with appropriate charge balance being maintained by an appropriate number of cation vacancies. However, such a simple model would introduce face-sharing of SnO_6 and FeO_6 octahedra which would be expected to be unstable due to high cation repulsions; in SnO_2 (rutile

0022-4596/97 $25.00

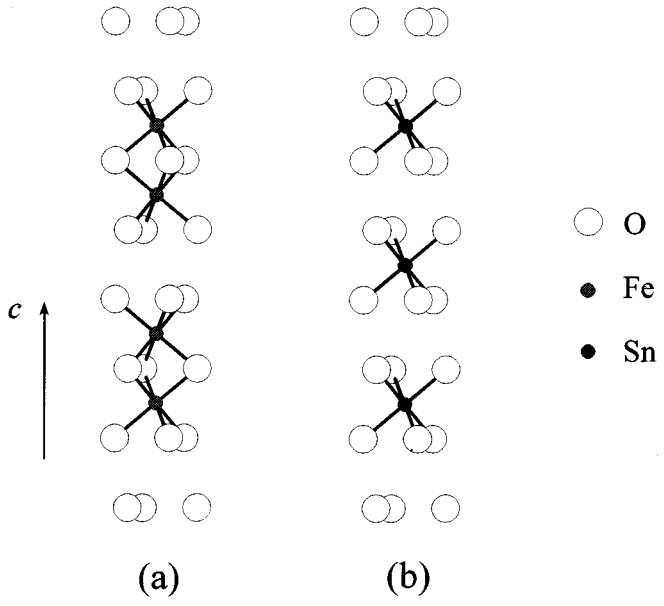

FIG. 1. Linking of FeO_6 octahedra along c in α-Fe_2O_3. (b) Structural model involving the substitution of $4Fe^{3+}$ ions by $3Sn(Ti)^{4+}$ ions.

structure) only edge- and corner-shared octahedra occur. An interesting difference between the Sn- and Ti-doped samples was revealed by simple refinements based on the α-Fe_2O_3 structure (space group R-3c) in which no cation substitution was involved, but the Fe site occupancy was allowed to vary. Whereas an apparent 10% reduction in Fe occupancy was indicated for the Ti-doped sample, the two Sn-containing materials showed a slight increase, although this was small (ca. 5%) even for the heavily substituted sample. Consideration of the atomic scattering factors—$f_{Sn} \sim 2_{Fe}$, $f_{Ti} < f_{Fe}$—provides a strong indicator that Sn/Ti occupancy of the Fe sites is occurring. Moreover, the data from the Sn-containing samples suggests approximately equal concentrations of Sn and vacancies on the Fe sites. Interestingly, this is inconsistent with a simple substitution model since the presence of three Sn^{4+} ions would be balanced by one vacancy.

Further refinements addressed an alternative model in which Sn partially occupies the octahedral sites that are vacant in pure α-Fe_2O_3 and are situated at the origin (0, 0, 0) in the unit cell. Sn(Ti) substitutions at Fe sites were not considered and charge balance was therefore maintained by the presence of four cation vacancies for every three Sn(Ti) ions introduced. The refinements provided clear evidence for the occupancy of these interstitial sites, but the occupancies were only approximately one third of those expected for the sample compositions. It was therefore apparent that the true structural model must involve both interstitial *and* substitutional Sn(Ti). The presence of Sn(Ti) in the interstitial sites would produce strong cation–cation repulsions from the two adjacent face-shared FeO_6 octahedra. Elimination of cations from these two sites results in two additional octahedral sites (respectively, above and below the cations removed) which do not involve face-sharing and therefore are attractive for occupation by additional Sn(Ti) atoms. In this way, the structural model of Fig. 1b was deduced: defect clusters are formed comprising a chain of three Sn(Ti) atoms which all avoid face-sharing repulsions. In addition, the cluster is electrically neutral since $4Fe^{3+}$ ions are replaced by $3Sn(Ti)^{4+}$ ions. With respect to the Fe sublattice, four Fe atoms are replaced by two Sn(Ti) atoms and two vacancies, in accord with the suggestions of the above refinements, which suggested approximately equal concentrations of Sn(Ti) and vacancies on this sublattice.

Refinements based on the above model provided very good fits for all three samples, Fig. 2, and the refined structural parameters are shown in Table 1. Effectively, only one occupancy was varied (that for Sn(Ti)2, in the interstitial site) since this determines the other cation site occupancies as indicated in Table 1. Due to correlation between the Sn(Ti) isotropic temperature factor and the site occupancy, in the final refinements the Sn(Ti) temperature factor was constrained to the realistic value of 1.0 $Å^2$. The refined temperature factor for Fe is large for α-$Fe_{1.67}Sn_{0.33}O_3$ and reflects the highly variable environment for Fe expected for such a highly substituted material. It should be noted that for this sample, the low angle part of the pattern, Fig. 2b, was excluded from the refinement, since the undulating background could not be modeled satisfactorily.

In addition to providing a very good fit to the experimental XRD data, the proposed structural model also gives Sn(Ti) contents which are in satisfactory agreement with analytical values (Table 1). Moreover, the defect model is based on sound chemical principles. The rutile structure, adopted by SnO_2 and TiO_2, can be envisaged as a distorted hexagonal close-packed arrangement of O^{2-} ions with Sn^{4+} ions occupying half the octahedral sites in an ordered fashion. Chains of face-shared octahedra exist perpendicular to the close-packed oxygen layers, as in α-Fe_2O_3, but in this structure alternate sites are occupied which totally eliminates face-sharing of SnO_6 octahedra. The clusters of 3Sn(Ti) proposed here for the substituted α-Fe_2O_3 samples are therefore microstructural regions of the rutile structure, the preferred structure of the substituting cations. Such clusters can be introduced into the α-Fe_2O_3 structure without any other disruption to the arrangement of Fe atoms within this lattice. The major change in atomic coordinates accompanying Sn(Ti) substitution involves the O^{2-} ions. Whereas in α-Fe_2O_3 this is situated at (0.306, 0, 0.25) (14), the x coordinate in the substituted samples appears to increase gradually to $x = 0.344$ for $Fe_{1.67}Sn_{0.33}O_3$. Referring to Fig. 1, this coordinate relates to the size of the triangles of O^{2-} ions which separate the adjacent Fe^{3+} ions. For

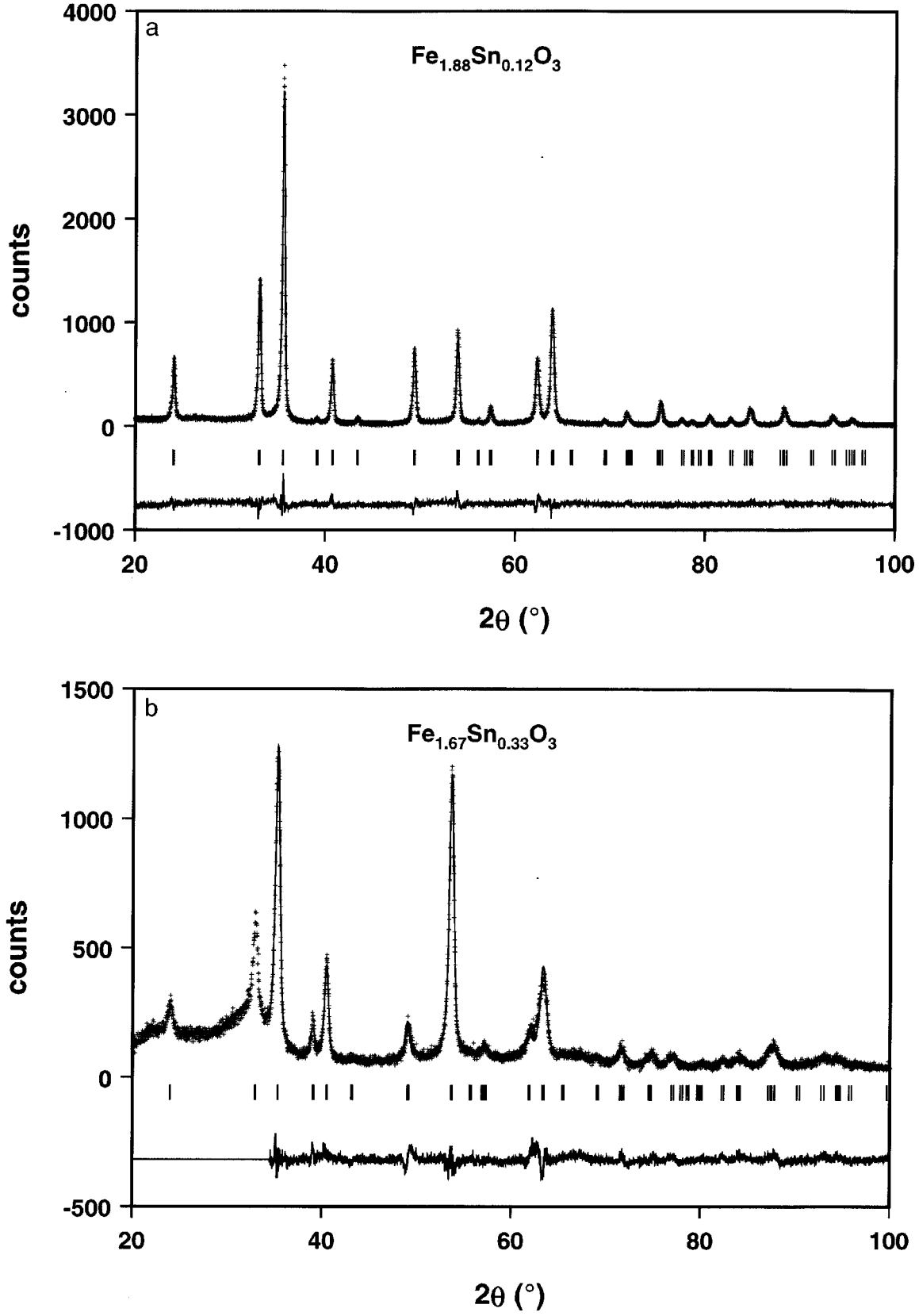

FIG. 2. Observed (+), calculated, and difference profiles, with reflection positions (|) for (a) α-$Fe_{1.88}Sn_{0.12}O_3$, (b) α-$Fe_{1.67}Sn_{0.33}O_3$, and (c) α-$Fe_{1.78}Ti_{0.22}O_3$.

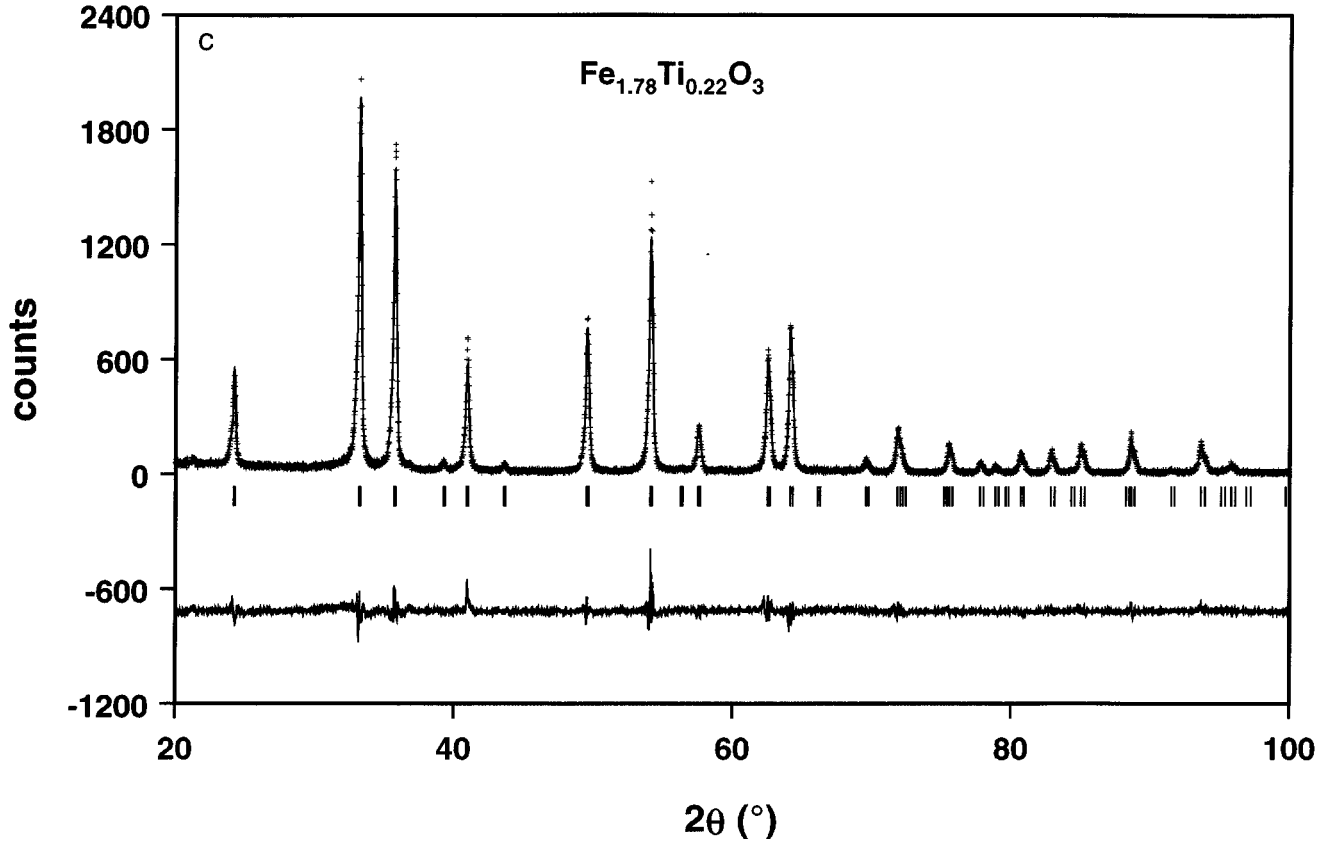

FIG. 2—*Continued*

TABLE 1
Refined Atomic Parameters from Powder X-Ray Diffraction [*R*-3*c*; O(x, 0, 1/4), Fe(0, 0, z), Sn(Ti)1 (0, 0, z), Sn(Ti)2 (0, 0, 0)]

		$Fe_{1.88}Sn_{0.12}O_3$	$Fe_{1.67}Sn_{0.33}O_3$	$Fe_{1.78}Sn_{0.22}O_3$
O	x/a	0.3108(9)	0.344(2)	0.313(1)
	B(Å^2)	1.8(1)	1.1(2)	1.15(8)
	Occupancy	18	18	18
Fe	z/c	0.3545(4)	0.351(2)	0.355(1)
	B(Å^2)	2.27(8)	6.4(3)	1.60(7)
	Occupancy[a]	11.24(4)	8.52(8)	10.36(8)
Sn(Ti)1	z/c	0.351(6)	0.344(2)	0.35(2)
	B(Å^2)	1.0	1.0	1.0
	Occupancy[a]	0.38(2)	1.74(4)	0.82(4)
Sn(Ti)2	B(Å^2)	1.0	1.0	1.0
	Occupancy[a]	0.19(1)	0.87(2)	0.41(2)
a (Å)		5.0408(5)	5.088(2)	5.0301(4)
c (Å)		13.780(2)	13.842(5)	13.7754(9)
R_{wp}[b] (%)		14.4	12.9	14.4
R_{exp}[b] (%)		9.5	9.3	10.8
R_I[b] (%)		7.0	6.6	5.1
% Sn/Ti (analysis)		6.3	16.4	11.3
% Sn/Ti (XRD)		4.8(3)	23(1)	10.6(5)

[a] Unit cell occupancy: Sn(Ti)1 = 2Sn(Ti)2; 12Fe = 4Sn(Ti)2.

[b] R_{wp} and R_{exp} have their usual significance in Rietveld analysis, but relate only to the parts of the profile at which Bragg peaks contribute. R_I is the integrated intensity agreement factor.

face-sharing octahedra, the anions tend to move together to minimize the cation–cation repulsions. For the substituted samples, the extent of face-sharing decreases with Sn(Ti) concentration, since the $Sn(Ti)O_6$ octahedra in the clusters, and the FeO_6 octahedra above and below the clusters, no longer share faces. The anions can therefore relax outward, which corresponds to an increase in x, as observed. It should also be noted that the change in unit cell size observed in the substituted samples (for α-Fe_2O_3 $a = 5.035$ Å, $c = 13.751$ Å (14)) simply reflects the octahedral cationic radii: Fe^{3+}, 0.65 Å; Ti^{4+}, 0.61 Å; Sn^{4+}, 0.69 Å (15).

ACKNOWLEDGMENT

We thank the EPSRC for the award of a studentship (JGM).

REFERENCES

1. F. J. Morin, *Phys. Rev.* **83,** 1005 (1951).
2. N. Uekawa, M. Watanabe, K. Kaneko, and F. Mizukami, *J. Chem. Soc., Faraday Trans.* **91,** 2161 (1995).
3. P. B. Fabritchnyi, E. V. Lamykin, A. M. Babechkin, and A. N. Nesmeianov, *Solid State Commun.* **11,** 343 (1972).
4. F. Schneider, K. Melzer, H. Mehner, and G. Deke, *Phys. Stat. Sol.* (*a*) **39,** K115 (1977).
5. M. Takano, Y. Bando, N. Nakanishi, M. Sakai, and H. Okinaka, *J. Solid State Chem.* **68,** 153 (1987).
6. S. Music, S. Popovic, M. Metikos-Hukovic, and G. Gvozdic, *J. Mater. Sci. Lett.* **10,** 197 (1991).
7. H. Kanai, H. Mizutani, T. Tanaka, T. Funabiki, S. Yoshida, and M. Takano, *J. Mater. Chem.* **2,** 703 (1992).
8. E. De Grave, D. Chambaere, and L. H. Bowen, *J. Magn. Magn. Mater.* **30,** 349 (1983).
9. E. De Grave, L. H. Bowen, and S. B. Weed, *J. Magn. Magn. Mater.* **27,** 98 (1982).
10. S. A. Fysh and P. E. Clark, *Phys. Chem. Miner.* **8,** 257 (1982).
11. S. Music, S. Popovic, and M. Ristic, *J. Mater. Sci.* **24,** 2722 (1989).
12. M. Ristic, S. Popovic, M. Tonkovic, and S. Music, *J. Mater. Sci.* **26,** 4225 (1991).
13. J. Rodriguez-Carajal, "FULLPROF v.2.6.1", (ILL, France), 1994; based on the original code by R. A. Young, *J. Appl. Crystallogr.* **14,** 149 (1981).
14. L. W. Finger and R. M. Hazen, *J. Appl. Phys.* **51,** 5362 (1980).
15. R. D. Shannon, *Acta Crystallogr. A* **32,** 751 (1976)